ORIGINAL ARTICLE

Exploring cutting front profile in abrasive water jet machining of aluminum alloys

Shu Wang[1] · **Dong Hu**[1] · **Fengling Yang**[1] · **Chuanlin Tang**[1] · **Peng Lin**[1]

Abstract

As the only cold high-energy beam machining technology, abrasive water jet (AWJ) has a very broad application prospect in material manufacturing industry. However, the application of AWJ is limited by the machining accuracy it can be achieved. To get higher accuracy in the AWJ cutting process, a better understanding of the cutting front is necessary since the machining accuracy is decided by the cutting front of AWJ. In this paper, the influence of machining parameters on the cutting front profile has been investigated. Based on the investigation, the cutting front profile model has been built and verified. With this mathematical model, predicting the cutting front profile accurately according to the cutting conditions becomes feasible and practical, which further leads to higher precision cutting of AWJ.

Keywords Abrasive water jet · Cutting front profile · Curve fitting · Predictive model

1 Introduction

When water is pressurized to high pressure and discharged from a small orifice, a high-speed water jet is formed. The abrasive water jet (AWJ) is formed by adding abrasive particles into the high-speed water jet [1]. All kinds of materials can be cut by using AWJ. As the only cold high-energy beam machining technology, AWJ has many advantages, so it is widely used in the material processing industry. Its advantages include no heat effect, no pollution to the environment, and high efficiency [2]. According to the existing data, it is clear that in many industrial fields, this technology can be used to cut parts with tolerances less than 0.1 mm, but the cutting accuracy cannot be further improved.

In the process of AWJ cutting, the jet is deflected opposite to the direction of the motion. That is to say, the exit of the jet from the material lags behind the point at the top of the material where the jet enters [3]. The jet-material interface is called the cutting front (as shown in Fig. 1). Unlike those traditional manufacturing methods, in which the machining accuracy is decided by the shape of tool, AWJ's

machining accuracy is decided by the cutting front of AWJ [4]. Therefore, it is necessary to further explore the behavior of the cutting front [5].

Many research scholars have conducted research on AWJ cutting front and have achieved many research results. Hashish recorded the cutting process of transparent materials using a high-speed camera and then studied the formation mechanism of the jet lag and cutting front [6]. Matsui et al. analyzed the cutting front and found that the arc can be used to represent the contour of cutting front, and the relationship between cutting speed and radius of arc was discussed [7]. Zeng et al. studied the AWJ cutting process and found that the parabola can be used to describe the contour of cutting front [8]. Kitamura et al. found that there is a linear relationship between the cutting speed and the jet lag, and when the thickness of the target material is increased, the slope will also increase [9]. Hashish's experimental data also confirmed this phenomenon [10]. Henning et al. found that the attenuation of abrasive particle energy has a great influence on the curvature of the cutting front [11]. Gostimirovic et al. studied the cutting parameters and optimized the curvature of the cutting front in AWJ machining from the perspective of abrasive mass flow rate and cutting speed [12]. Akkurt pointed out that because of the energy loss of the jet, the cutting front is formed by deviation from the ideal geometry, and the second-order parabolic function can be used to represent the cutting front profile

✉ Dong Hu
  hudong_9@126.com

1 School of Energy and Electromechanical Engineering, Hunan University of Humanities, Science and Technology, Loudi, China
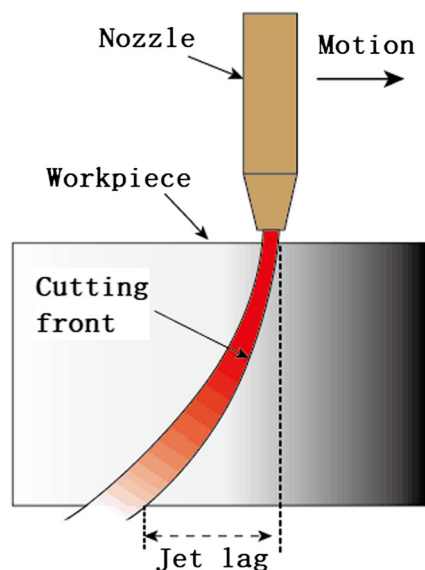
Fig. 1 Cutting front

Fig. 2 Bridge generated in separation process

2 Experimental study

It is clear that when the cutting parameters are changed, the performance of the AWJ cutting front will be changed. In order to study the relationships between the cutting front profiles and the processing parameters, experimental research is required.

The material chosen for this paper is aluminum alloy 6061 T, which is widely used in the industrial field. The nominal chemical composition of the material includes the following: Al content is 97.75%, Ti content is 0.05%, Zn content is 0.07%, Cr content is 0.06%, Mg content is 0.85%, Mn content is 0.32%, Cu content is 0.22% , and Si content is 0.68%. Its machinability index in AWJ is 219.3, the Young's modulus for it is 69 GPa, and the yield strength is 405 MPa. Because the parameters such as abrasive size and abrasive type are usually unchanged, they are not considered in this paper. Table 1 shows the variable factors in this experiment, including the target material thickness, cutting surface quality, water pressure, and abrasive flow rate.

In order to allow the sample to be sufficient, five levels of target material thickness, and three levels of cutting surface quality, water pressure, and abrasive flow rate were tested. In Table 1, the cutting surface quality represents nozzle traverse speed. The higher the cutting surface quality, the slower the nozzle traverse speed and the smoother the cutting surface [17]. Q3, Q5, and Q10 are named as cutting surface quality number, and they represent different nozzle traverse speed levels. It needs to be clear that in order to improve the accuracy of cutting, the quality level of the cutting surface was
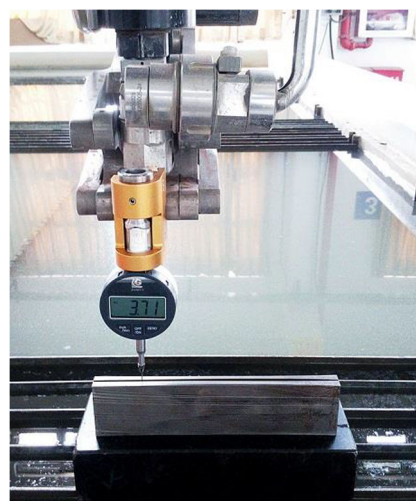
[13]. After in-depth research, Zhang et al. also proved this phenomenon [14]. Jerman et al. studied the cutting front development using a two-dimensional cellular automata model and described the cutting process by simplified material removal and AWJ propagation models in the form of cellular automata rules [15]. Mital et al. used a 3D laser profiler to measure the AWJ's kerf surface, and based on this, they created 3D images [16].

The above efforts provided some very important information to understand AWJ cutting front. However, it still cannot meet the requirements of the higher tolerance cutting. To improve the accuracy of the cutting process, predicting what cutting front profile would be expected with selected parameters accurately is very important. This paper investigated the relationships between the cutting front profiles and the processing parameters. Based on this, a cutting front profile model has been constructed and verified.

Table 1 Experimental parameters list

Parameters	Specifications
Target material thickness (mm)	10, 25, 50, 100, 150
Cutting surface quality	Q3, Q5, Q10
Water pressure (MPa)	245, 315, 385
Abrasive flow rate (kg/min)	0.25, 0.35, 0.45
Standoff distance (mm)	1.5
Abrasive size (mesh)	100
Abrasive type	Garnet
Mixing tube diameter (mm)	0.889
Orifice diameter (mm)	0.33
Target material	Al-6061 T

Fig. 3 The equipment for measuring the cutting front profile
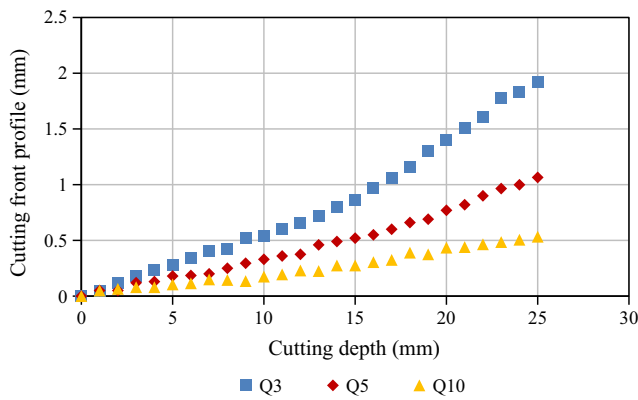
Fig. 4 Nozzle traverse speed affects cutting front profile (the abrasive flow rate is 0.25 kg/min, the water pressure is 315 MPa, and the sample thickness is 25 mm)

Fig. 6 Example of curve fitting (the cutting surface quality is Q10, the sample thickness is 150 mm, the water pressure is 245 MPa, and the abrasive flow rate is 0.45 kg/min)

selected from Q3, which corresponds to the lower nozzle movement speed. The relationship between cutting surface quality number and cutting speed is obtained from the model of Zeng [18] as shown in the following:

$$U = \text{Usep}/Q^{1.15} \tag{1}$$

where U is the actual nozzle movement speed (mm/s), Usep is the separation speed (mm/s), and Q is the cutting surface quality level.

Separation speed is the maximum speed to cut through the target material. In order to obtain the separation speed, multiple trial cuts with discrete nozzle traverse speeds have been made on the same piece of target material until the separation speed based on a certain separation standard is found. The separation standard means that the sum of the remaining "bridges" width at the bottom of the incision is less than 1.6 mm (as shown in Fig. 2). After the separation speed is determined, the actual movement speed of the nozzle can be calculated using Eq. (1).

After the determination of the parameters is completed, the samples are prepared for experimental study. The width of the
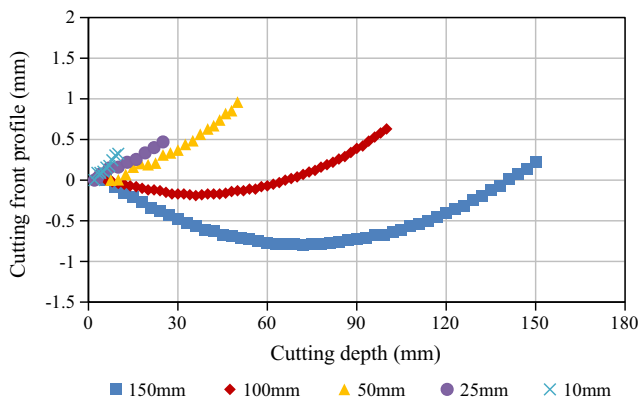
sample is 20 mm and the length is 50 mm. For each sample, a line in the middle is cut by AWJ. In order to obtain the cutting front information, it is necessary to pull out the abrasive feed hose from the side of the nozzle under the condition of stable cutting speed. Under this condition, abrasive particles are cut off as soon as the abrasive feeding hose is pulled out, and the cutting front can be obtained. After that, a digital dial indicator with a rigid needle fixed on it is used to measure the cutting front (as shown in Fig. 3). And then by moving the digital dial indicator along the cutting front, cutting front information can be obtained accurately.

3 Results and discussions

3.1 Influence of nozzle traverse speed on the cutting front profile

As shown in Fig. 4, the abrasive flow rate is 0.25 kg/min, the water pressure is 315 MPa, and the sample thickness is 25 mm. Under the condition of using the same nozzle, the curves produced by different moving speeds are different. Analysis of the curve makes it clear that for the contour of cutting front,

Fig. 5 Target material thickness affects cutting front profile (the abrasive flow rate is 0.45 kg/min, the water pressure is 315 MPa, and the cutting surface quality is Q10)
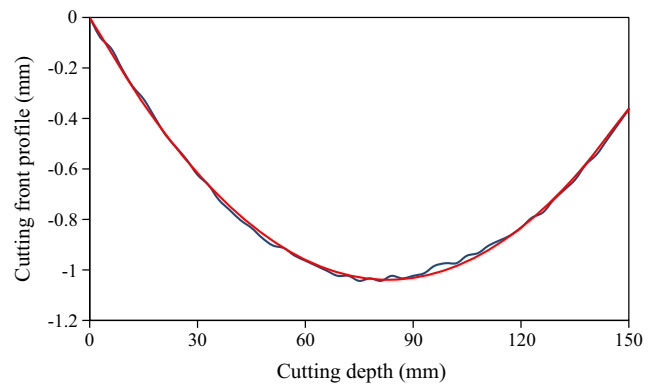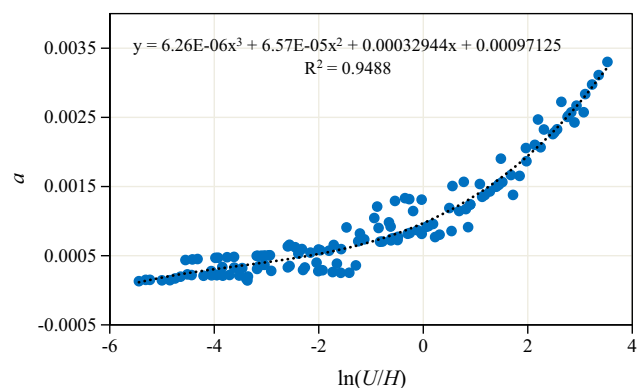

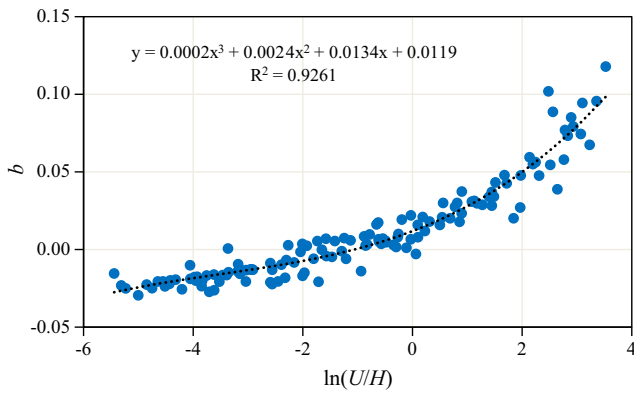**Fig. 7** Relation of a vs. $\ln(U/H)$

Fig. 8 Relation of b vs. $\ln(U/H)$

the nozzle movement speed has a greater influence on it. The faster the nozzle moves, the greater the jet lag becomes.

3.2 Influence of target material thickness on the cutting front profile

As shown in Fig. 5, the abrasive flow rate is 0.45 kg/min, the water pressure is 315 MPa, and the cutting surface quality is Q10. Under the condition of using the same cutting parameters, different target material thickness produces different curves. Analysis of the curve makes it clear that the target material thickness has a greater influence on the contour of cutting front. If the target material thickness is larger, the middle part of the cutting front will gradually become convex, which will eventually lead to exceeding the injection point of the jet into the material.

4 Predictive model for the cutting front profile curve

4.1 Model building

There are 135 curves obtained in this paper. It is clear from the analysis that these data can be fitted with parabolic curves, and the square of the correlation coefficient for all fittings is greater than 0.95. Therefore, it can be considered that when fitting the contour of cutting front, a parabolic curve can be used.
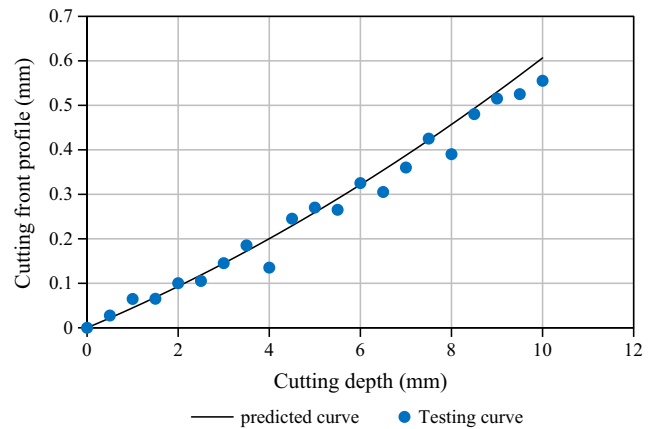

Fig. 9 Compare the test curve with the predicted curve (Test 1, the nozzle traverse speed is 57 mm/min, the abrasive flow rate is 0.225 kg/min, the water pressure is 385 MPa, and the target material thickness is 10 mm)

Therefore, this paper describes the cutting front profile curve as:

$$J(h) = ah^2 + bh \tag{2}$$

where h is the cutting depth (mm) and a and b are regression coefficients.

Figure 6 shows the curve fitting diagram. In Fig. 6, the fitting curve is represented by a red smooth curve, and the actual data is represented by a blue irregular curve. The Levenberg-Marquardt algorithm is the fitting method used. The fitting parameters are listed as follows:

a: 0.000151004890009949
b: -0.0250534872831668
RMSE: 0.011927846585149
SSE: 0.00725594973210134
R: 0.999116748102848
R^2: 0.998234276339609
DC: 0.998233072773634
Chi-Square: -0.00644526834749448
F Statistic: 27701.6617253768

The research results show that there are two factors that have an important influence on the cutting profile;

Table 2 Verification test parameters

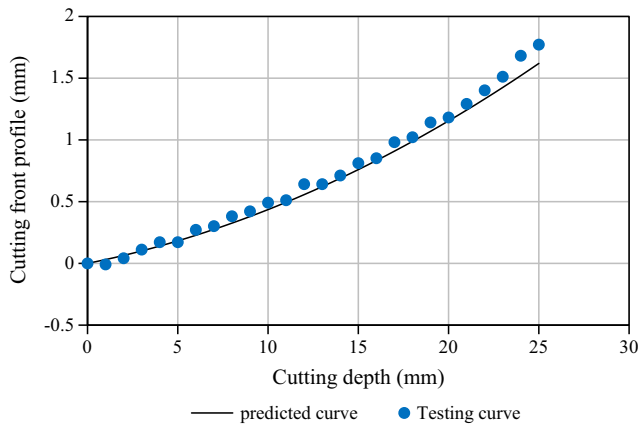| Parameters	Abrasive flow rate (kg/min)	Water pressure (MPa)	Target material thickness (mm)	Nozzle traverse speed (mm/min)
Test 1	0.225	385	10	57
Test 2	0.225	385	25	75
Test 3	0.458	385	50	50
Test 4	0.458	315	100	14
Test 5	0.458	245	150	3.27

Fig. 10 Compare the test curve with the predicted curve (Test 2, the nozzle traverse speed is 75 mm/min, the abrasive flow rate is 0.225 kg/min, the water pressure is 385 MPa, and the target material thickness is 25 mm)

one is the target material thickness, and the other is the nozzle moving speed, although other factors also affect the cutting front profile, such as abrasive flow rate, water pressure. However, when these parameters are changed, the nozzle movement speed will inevitably be changed, so when researching, just study the nozzle movement speed directly.

The research shows that there is a good relationship between the regression coefficients and ln(U/H), and the relationship can be expressed using a cubic polynomial, as shown in Figs. 7 and 8.

On the basis of completing the data test, the following formula can be used to express the relationship between the regression coefficients and ln (U/H):

$$a = 0.00000626\ln^3(U/H) + 0.00006571\ln^2(U/H)$$
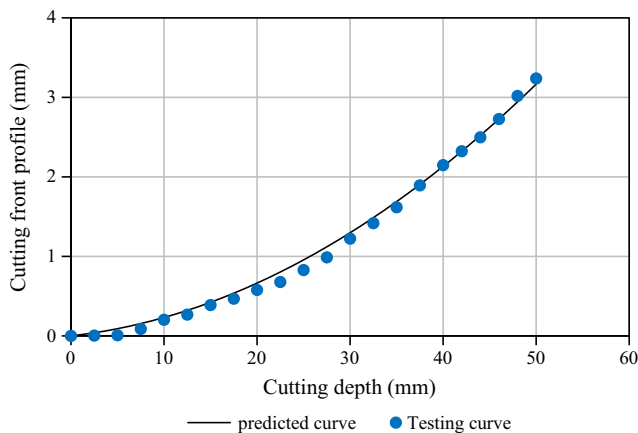$$+0.00032944\ln(U/H) + 0.00097125 \quad (3)$$

Fig. 11 Compare the test curve with the predicted curve (Test 3, the nozzle traverse speed is 50 mm/min, the abrasive flow rate is 0.458 kg/min, the water pressure is 385 MPa, and the target material thickness is 50 mm)
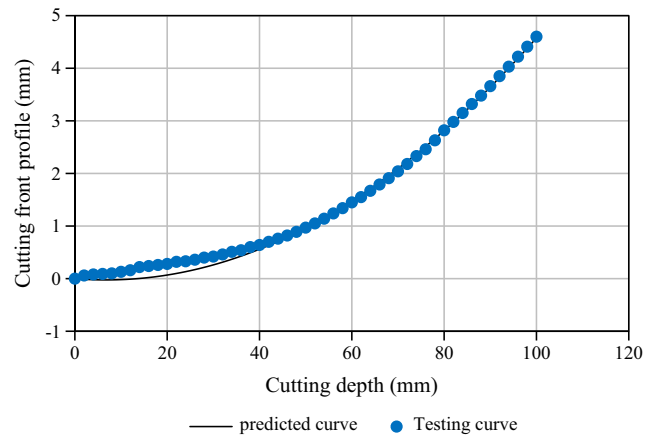

Fig. 12 Compare the test curve with the predicted curve (Test 4, the nozzle traverse speed is 14 mm/min, the abrasive flow rate is 0.458 kg/min, the water pressure is 315 MPa, and the target material thickness is 100 mm)

$$b = 0.00022495\ln^3(U/H) + 0.0023621\ln^2(U/H)$$
$$+0.013428\ln(U/H) + 0.011852 \quad (4)$$

Substituting Eq. (3 and 4) into Eq. (2) leads to

$$J(h) = \left[0.00000626\ln^3(U/H) + 0.00006571\ln^2(U/H) + 0.00032944\ln(U/H) + 0.00097125\right]h^2 + \left[0.00022495\ln^3(U/H) + 0.0023621\ln^2(U/H) + 0.013428\ln(U/H) + 0.011852\right]h \quad (5)$$

The moving speed of the nozzle can be clarified from the Zeng's model [19], so there are:

$$U = \left(\frac{N_m P_w^{1.25} \dot{m}_w^{0.687} \dot{m}^{0.343}}{C_s Q H D^{0.618}}\right)^{1.15} \quad (6)$$

where U is the nozzle movement speed (mm/s), N_m is the machinability number of material, P_w is the water pressure
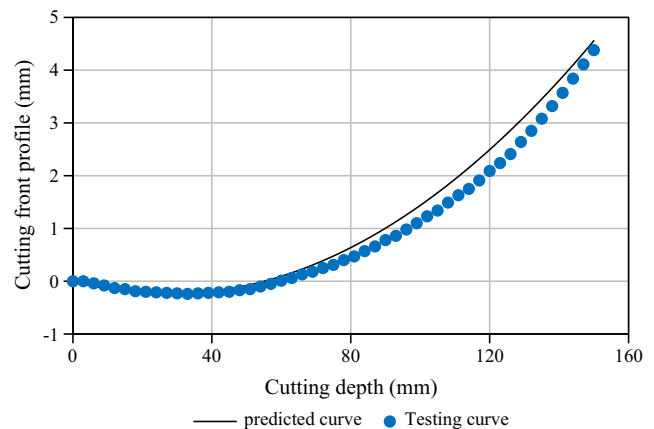

Fig. 13 Compare the test curve with the predicted curve (Test 5, the nozzle traverse speed is 3.27 mm/min, the abrasive flow rate is 0.458 kg/min, the water pressure is 245 MPa, and the target material thickness is 150 mm)

(MPa), $\dot{m}_w$ is the water flow rate (lpm), $\dot{m}$ is the abrasive flow rate (g/s), C_s is the scale factor, Q is the cutting surface quality, H is the sample thickness (mm), and D is the mixing tube diameter (mm).

Analyzing the equation, the waterjet machine tool and the target material will affect some parameters. In this experiment, this parameter has a fixed value. Therefore, these parameters can be regarded as constants, which make the fitting easier, so there are:

$$U = \frac{rP^{1.4375}m^{0.39445}}{C_T H^{1.15}} \tag{7}$$

where r is the ratio of nozzle movement speed (the ratio of nozzle movement speed over separation speed), P is the water pressure (MPa), and m is the abrasive flow rate (g/s).

The value of C_T can be calculated by the following formula

$$C_T = \left(\frac{C_S D^{0.618}}{N_m \dot{m}_w^{0.687}}\right)^{1.15} \tag{8}$$

By collating Eq. (5) and Eq. (7), the prediction model of the cutting front profile can be obtained as:

$$
\begin{aligned}
J(h) = &\left[0.00000626\ln^3\left(\frac{rP^{1.4375}m^{0.39445}}{C_T H^{2.15}}\right) + 0.00006571\ln^2\left(\frac{rP^{1.4375}m^{0.39445}}{C_T H^{2.15}}\right)\right.\\
&\left. + 0.00032944\ln\left(\frac{rP^{1.4375}m^{0.39445}}{C_T H^{2.15}}\right) + 0.00097125\right]h^2\\
&+ \left[0.00022495\ln^3\left(\frac{rP^{1.4375}m^{0.39445}}{C_T H^{2.15}}\right) + 0.0023621\ln^2\left(\frac{rP^{1.4375}m^{0.39445}}{C_T H^{2.15}}\right)\right.\\
&\left. + 0.013428\ln\left(\frac{rP^{1.4375}m^{0.39445}}{C_T H^{2.15}}\right) + 0.011852\right]h
\end{aligned}
\tag{9}
$$

4.2 Model validation

In order to evaluate the model, it is therefore tested. Table 2 shows the cutting parameters. Figures 9, 10, 11, 12 and 13 show the relationship between the test data and the prediction curve. The Pearson correlation coefficients between the test curve and the predicted curve are 0.9918, 0.9985, 0.9993, 0.9987, and 0.9974. So it can be clear that, based on the given cutting conditions, the prediction model can be used to predict the cutting front curve.

5 Conclusions

The results of this study show that:

The movement speed of the nozzle and the thickness of the target material have great influences on the contour of the cutting front. The faster the nozzle moves, the greater the jet lag becomes. As the material thickness increases, the middle part of the cutting front will gradually become convex, which

will eventually lead to exceeding the injection point of the jet into the material. In addition, some other parameters (such as abrasive flow rate, water pressure, etc.) will definitely affect the contour of cutting front, but changes in these parameter values will lead to changes in nozzle movement speed. Therefore, there is no need to consider those parameters separately.

It is clear from the experimental data that when fitting the cutting front profile, a parabola can be used. Therefore, in this paper, the parabolic fitting technique is used to determine the prediction model, and the model is used to predict the cutting front profile under different AWJ cutting conditions. As a result, a better understanding of AWJ cutting process can be achieved. This would provide a reference for improving the accuracy of AWJ.

References

1. Chen M, Zhang S, Zeng J, Chen B, Xue J, Ji L (2019) Correcting shape error on external corners caused by the cut-in/cut-out process in abrasive water jet cutting. Int J Adv Manuf Technol 103(1-4): 849–859
2. Chen M, Zhang S, Zeng J, Chen B (2019) Correcting shape error located in cut-in/cut-out region in abrasive water jet cutting process. Int J Adv Manuf Technol 102(5–8):1165–1178
3. Hashish M (2006) Enhanced abrasive waterjet cutting accuracy with dynamic tilt compensation. CRIP 2nd International Conference on High Performance Cutting, Vancouver, British Columbia, 12–13 June 2006
4. Zhang S, Wu Y, Wang S (2015) An exploration of an abrasive water jet cutting front profile. Int J Adv Manuf Technol 80(9–12): 1685–1688
5. Henning A, Westkämper E (2006) Analysis of the cutting front in abrasive waterjet cutting. Proceedings of the 18th international conference on water jetting, Gdansk, pp 425–434
6. Hashish M (1988) Visualization of the abrasive waterjet cutting process. Exp Mech 28(2):159–169
7. Matsui S, Matsumura H, Ikemoto Y, Tsujita K, Shimizu H (1990) High precision cutting method for metallic materials by abrasive waterjet. Proceedings of the 10th International Symposium, Amsterdam, pp 263–278
8. Zeng J, Heines R, Kim TJ (1991) Characterization of energy dissipation phenomenon in abrasive waterjet cutting. Proceedings of the 6th American waterjet conference, Houston, Texas, pp 163–177
9. Kitamura M, Ishikawa M, Sudo K (1992) Cutting of steam turbine components using an abrasive water jet. Jet Cut Technol. Springer Netherlands 1992:543–554
10. Hashish M (2007) Benefits of dynamic waterjet angle compensation. 2007 American WJTA Conference and Expo, Houston, Texas, 1-H
11. Henning A, Westkamper E, Schmidt B (2004) Analysis of geometry at abrasive waterjet cutting operation. Proceedings of the 17th international conference on water jetting-advances and future needs, Mainz, pp 465–474

12. Gostimirovic M, Pucovsky V, Sekulic M, Rodic D, Pejic V (2019) Evolutionary optimization of jet lag in the abrasive water jet machining. Int J Adv Manuf Technol 101:3131–3141

13. Akkurt A (2010) Cut front geometry characterization in cutting applications of brass with abrasive water jet. J Mater Eng Perform 19(4):599–606

14. Wu Y, Zhang S, Wang S, Yang F, Tao H (2015) Method of obtaining accurate jet lag information in abrasive water-jet machining process. Int J Adv Manuf Technol 76(9-12):1827–1835

15. Jerman M, Valentincic J, Lebar A, Orbanic H (2015) The study of abrasive water jet cutting front development using a two-dimensional cellular automata model. Strojniski Vestnik 61(5): 292–302

16. Mital G, Dobránsky J, Ružbarský J, Olejárová Š (2019) Application of laser profilometry to evaluation of the surface of the workpiece machined by abrasive waterjet technology. Appl Sci 9(10):2134

17. Zeng J (2007) Determination of machinability and abrasive cutting properties in AWJ cutting. 2007 American WJTA Conference and Expo, Houston, Texas, pp 19–21

18. Zeng J, Kim TJ, Wallace RJ (1992) Quantitative evaluation of machinability in abrasive waterjet machining. 1992 Winter Annual Meeting of ASME, "Precision Machining: Technology and Machine Development and Improvement", PED-Vol.58, Anaheim, pp 169–179

19. Zeng J (1992) Mechanisms of brittle material erosion associated with high pressure abrasive waterjet processing-a modeling and application study. University of Rhode Island, Dissertation